A Novel Approach to Predicting P450 Mediated Drug Metabolism. CYP2D6 Catalyzed N-Dealkylation Reactions and Qualitative Metabolite Predictions Using a Combined Protein and Pharmacophore Model for CYP2D6

Marcel J. de Groot,*,‡ Mark J. Ackland,† Valerie A. Horne,‡ Alexander A. Alex,‡ and Barry C. Jones†

Departments of Molecular Informatics, Structure and Design and Drug Metabolism, Pfizer Central Research, Sandwich, Kent CT13 9NJ, United Kingdom

Received April 12, 1999

A combined protein and pharmacophore model for cytochrome P450 2D6 (CYP2D6) has been extended with a second pharmacophore in order to explain CYP2D6 catalyzed N-dealkylation reactions. A group of 14 experimentally verified N-dealkylation reactions form the basis of this second pharmacophore. The combined model can now accommodate both the usual hydroxylation and O-demethylation reactions catalyzed by CYP2D6, as well as the less common N-dealkylation reactions. The combined model now contains 72 metabolic pathways catalyzed by CYP2D6 in 51 substrates. The model was then used to predict the involvement of CYP2D6 in the metabolism of a "test set" of seven compounds. Molecular orbital calculations were used to suggest energetically favorable sites of metabolism, which were then examined using modeling techniques. The combined model correctly predicted 6 of the 8 observed metabolites. For the well-established CYP2D6 metabolic routes, the predictive value of the current combined protein and pharmacophore model is good. Except for the highly unusual metabolism of procainamide and ritonavir, the known metabolites not included in the development of the model were all predicted by the current model. Two possible metabolites have been predicted by the current model, which have not been detected experimentally. In these cases, the model may be able to guide experiments. P450 models, like the one presented here, have wide applications in the drug design process which will contribute to the prediction and elimination of polymorphic metabolism and drug−drug interactions.

Introduction

Cytochrome P450 2D6 (CYP2D6[1]) is a polymorphic member of the P450 superfamily which is absent in 5−9% of the Caucasian population,[2] resulting in a deficiency in drug oxidation known as the debrisoquine/sparteine polymorphism. The well-known substrates of CYP2D6 represent a variety of chemical structures, common characteristics being the presence of at least one basic nitrogen atom, a distance of 5, 7, or 10 Å between the basic nitrogen atom and the site of oxidation, a flat hydrophobic area near the site of oxidation, and a negative molecular electrostatic potential (MEP) above the planar part of the molecule.[3−7]

Theoretical models capable of predicting the possible involvement of CYP2D6 in the metabolism of drugs or drug candidates are important tools for use in drug discovery and drug development. Several pharmacophore models have been published based on the chemical structure of a variety of substrates or reversible inhibitors.[3−5,8−12] Furthermore, protein models of CYP2D6[6,13−17] have been constructed using the crystal structure of either CYP101,[18,19] CYP102,[20,21] or a combination of CYP101, CYP102, and CYP108.[22] For a review of these models see de Groot and Vermeulen.[23]

Recently, a combined model for CYP2D6[7] was derived based on the combination of a homology model constructed using the crystal structures of CYP101, CYP102, and CYP108, a pharmacophore model, and molecular orbital (MO) calculations on the substrates, metabolic intermediates, and products. This methodology[7] offers a more complete understanding of the CYP2D6 active site and its interactions with substrates than each of these approaches alone, since it takes into account the most reactive sites in the substrate, as well as the conformational and stereochemical constraints imposed by the protein active site. The independent generation of the pharmacophore and protein models offered the opportunity to "cross-validate" the approaches used.

CYP2D6 catalyzed N-dealkylation was initially considered an atypical and rare pathway, but as more and more compounds were found to be N-dealkylated by CYP2D6 it has become an accepted metabolic pathway.[24] The first aim of the present study is to add a pharmacophore for N-dealkylation reactions catalyzed by CYP2D6 to the combined model for CYP2D6.[7] A separate pharmacophore model is necessary as the existing pharmacophore models all indicate that metabolism catalyzed by CYP2D6 should occur at a distance of 5, 7, or 10 Å away from the basic nitrogen atom, not directly adjacent to it.[3,5,7−12] A set of 14 substrates for which experimental evidence is available for the involvement of CYP2D6 in the N-dealkylation was selected for this purpose.

The second aim of the present study is to challenge our recently derived three-dimensional model of CYP2D6,[7] including the new pharmacophore for N-dealkylation reactions, in terms of its ability to predict the metabolism of a set of seven test compounds.[25]

* Corresponding author.
‡ Department of Molecular Informatics, Structure and Design.
† Department of Drug Metabolism.

10.1021/jm991058v CCC: $18.00
Published on Web 09/09/1999

No information was available to us at the time of the predictions in terms of actual sites of oxidation. After these predictions were made, a comparison between predictions and experimental results from the literature was performed. These results have to be examined carefully as there are several results possible for each substrate: (*a*) correct prediction of a known metabolite, (*b*) prediction of a metabolite that has not (yet) been detected experimentally, (*c*) prediction of a metabolite that is *not* formed, (*d*) failure to predict a known metabolite. Preferably, the model should identify all experimentally detected metabolites and not predict metabolites that are not formed. Metabolites predicted by the model that have not (yet) been identified experimentally have to be confirmed with the appropriate experiments in order to determine whether the model made incorrect predictions or the metabolites have so far eluded detection. Should the metabolites be detected experimentally, this would indicate the model's ability to guide experiments. The model is not yet capable of distinguishing between substrates and competitive inhibitors.

Computational Methods

Construction of a Pharmacophore Model for N-Dealkylation of Substrates of CYP2D6 and Molecular Orbital (MO) Calculations. For the 15 metabolic N-dealkylation pathways of the 14 substrates known to be metabolized by human CYP2D6, experimental information concerning their sites of oxidation were obtained from the literature (see Figure 1 and Table 1). The structures were built using SPARTAN.[26] For each of the compounds (Figure 1)[27] a conformational search followed by an energy minimization was performed[28] using the AM1-method[29] in SPARTAN.[26] Starting from the lowest energy minimized conformation of the molecule, all likely radicals and hydroxylated products and the radical cation were generated and geometry optimized.[30] MPTP (**46**) was selected as a template for the N-dealkylation pathway, as additional information on the approximate orientation in the CYP2D6 active site was available.[15,31] Each substrate was then overlaid onto MPTP or other substrates (see below) using the "MULTIFIT"[32] method in SYBYL.[33]

In the next step each individual substrate was energy minimized within the active site using SYBYL.[33] In this minimization only amino acids Glu216, Asp301, and Phe481 (experimentally identified or suggested by modeling as amino acids primarily responsible for interactions with substrates[7]) and the substrate were free to minimize, with a distance constraint[34] to keep the site of oxidation (see Figure 1, yellow arrows) near the iron atom. After fitting/docking the compound in the combined model and minimization of the compounds in the presence of the protein, an AM1 geometry optimization was performed on the resulting substrate structure in order to check that the conformations resulting from minimization within the protein are low-energy conformations and not sterically strained high-energy conformations.

Testing the Compounds in the Combined Model for CYP2D6 and Molecular Orbital (MO) Calculations on Potential CYP2D6 Substrates. For each of the compounds (Figure 2)[27] a conformational search

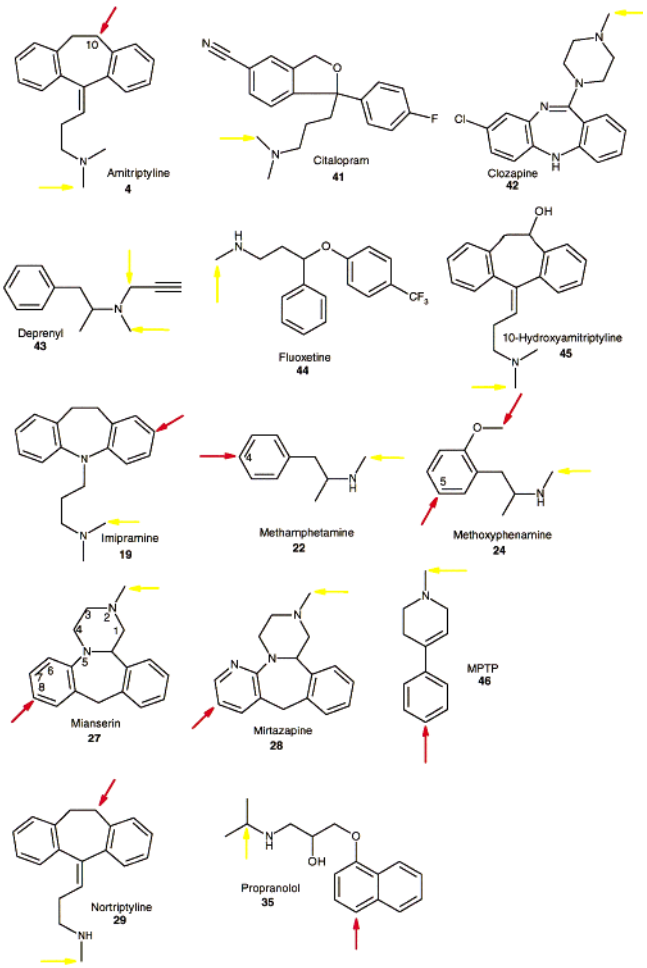

Figure 1. Compounds used to construct a pharmacophore model for N-dealkylation reactions catalyzed by CYP2D6 model, as an extension of the combined protein and pharmacophore model.[7] Known hydroxylation and O-demethylation reactions are indicated with red arrows (part of the initial pharmacophore[7]); known N-dealkylations are indicated by yellow arrows. In symmetry related cases only one site is indicated. The aromatic hydroxylation was not included in the initial pharmacophore model so far.

Table 1. CYP2D6 Substrates Showing N-Dealkylation and Their Metabolic Pathways

name	no.[7,27]	pathway(s)	ref
amitriptyline	**4**	N-demethylation	56−58
citalopram	**41**	N-demethylation	59
clozapine	**42**	N-demethylation	60
deprenyl	**43**	N-demethylation	61
		N-depropargylation	61
fluoxetine	**44**	N-demethylation	50
10-hydroxyamitriptyline	**45**	N-demethylation	56
imipramine	**19**	N-demethylation	62, 63
methamphetamine	**22**	N-demethylation	64
methoxyphenamine	**24**	N-demethylation	65
mianserine	**27**	N-demethylation	66
mirtazapine	**28**	N-demethylation	67
MPTP	**46**	N-demethylation	68
nortriptyline	**29**	N-demethylation	69
propranolol	**35**	N-desisopropylation	70, 71

followed by an energy minimization was performed as described above.[28] The MO calculations now play a more important role as predictions based on the model are made. As no experimental information is available for the compound under investigation, the MO results are used to guide the modeling. Guided by the relative

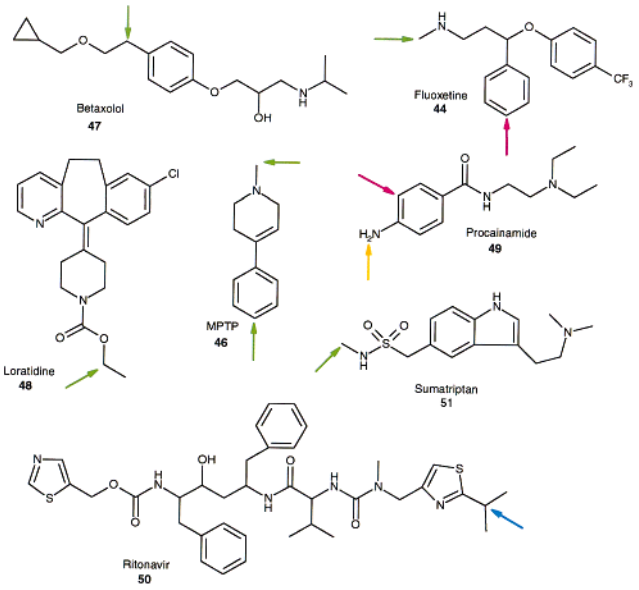

Figure 2. Compounds used to test the combined CYP2D6 model. Correctly predicted sites of metabolism are marked with a green arrow. Experimentally unverified predicted sites of metabolism are marked with a magenta arrow. The highly unusual site of metabolism in ritonavir (**50**) which could not be predicted but could be rationalized is indicated with a blue arrow. The N-hydroxylation product of procainamide (**49**) that could not be predicted by our current model is indicated with an orange arrow.

energies of the various possible products and the distances between suggested sites of metabolism and the basic nitrogen atom, the most likely sites of metabolism were selected. The fitting/docking of the compounds and the following SYBYL and AM1 calculations were performed in a similar way as described above for the construction of the N-dealkylation pharmacophore except for the two distance constraints[35] to ensure known interactions were preserved in the SYBYL optimization in the presence of the protein.

Each compound was overlaid using the previously described criteria[7] onto either debrisoquine or dextromethorphan depending on whether it was a 5 Å or 7 Å substrate as described above.[32] All predicted substrates were able to conform to the 7 Å model (7.3−8.4 Å), using dextromethorphan as the sole template molecule interacting with Asp301. The "7 Å substrates" from the "training set"[7] had distances between 6.4 and 8.8 Å between the site of oxidation and basic nitrogen atom.

Results and Discussion

Construction of a Separate Pharmacophore Model for N-Dealkylations within the Original Combined Pharmacophore and Protein Model. 1. Substrates Containing a Single Aromatic Ring. One of the orientations of MPTP (**46**) in the active site of CYP2D6,[36] as identified by NMR measurements,[15,31] was used as an initial starting point for orientating MPTP in the CYP2D6 active site. MPTP was reoriented slightly in the active site of our protein model[7] in order to get the aromatic ring close to the aromatic side chain of Phe481. Deprenyl (**43**, two orientations, one for each metabolite), *S*-methamphetamine (**22**), and methoxyphenamine (**24**) were superimposed onto MPTP (**46**), using the site of metabolism (N-dealkylation) and the aromatic rings for the superimposing using MULTIFIT. These five structures were then repositioned together in the active site in order to optimize the interaction between the aromatic rings and Phe481.[37,38] Constrained SYBYL minimizations in the protein were then initiated[34] which changed the orientations of the substrates only slightly. This superposition of substrates was now used to superimpose other substrates.

2. Substrates Containing Multiple Aromatic Rings. The remaining substrates that undergo CYP2D6 catalyzed N-dealkylations contain two aromatic rings. One of these rings was superimposed on the aromatic ring of **46**. The most rigid substrates were fitted first.

Mianserine (**27**) could be fitted onto **46** with one aromatic ring coplanar with Phe481, while the other aromatic ring of **27** was in an orientation interacting with the side chain of Leu121 (F-helix). The corresponding amino acid in CYP108 (Thr103) is also involved in protein−substrate interactions.[22] Mirtazapine (**28**) could be fitted in an identical orientation.

Amitriptyline (**4**) and 10-hydroxyamitriptyline (**45**) could be superimposed onto **46** in an orientation similar to that of **27**. Imipramine (**19**) was added to the pharmacophore by superimposing it on amitriptyline (**4**). Fluoxetine (**44**) was also added to the model by fitting it onto amitriptyline (**4**).

Propranolol (**35**) and clozapine (**42**) were superimposed onto **46**, while maximizing the overlap with **4**, **27**, **28**, and **45**. This identified an additional protein−substrate interaction for **42**. The chlorine containing ring is interacting with the side chain of Leu213. The corresponding amino acid has been identified as a residue responsible for substrate interactions in CYP2A4[39−42] and CYP2B1.[43−46]

Both the *R*- and the *S*-enantiomer of citalopram (**41**) could be accommodated in the N-dealkylation pharmacophore. The *R*-enantiomer was fitted with the fluorine containing ring on the aromatic ring of **46**, while in the case of the *S*-enantiomer, the double ring system of **41** was superimposed on the aromatic ring of **46**, while **27** was used as a guide for the superpositioning. The cyanide moiety of *S*-**41** interacted again with Leu213.

Although the aromatic rings interacting with Phe481 are very well overlaid, there is some freedom in the positioning of the second aromatic ring between different substrates.

3. Combining the Pharmacophore for N-Dealkylations with the Combined Pharmacophore and Protein Model for CYP2D6. The derived pharmacophore was merged with the original pharmacophore and protein model from our combined CYP2D6 model.[7] Figure 3 shows the incorporation of the N-dealkylation pathways (yellow) into the combined pharmacophore (red) and protein model (protein not shown for clarity), after the optimizations in the protein. The two pharmacophores can be combined, although the planar regions of the two pharmacophores do not coincide. This is mainly caused by different protein−substrate interactions for the two pharmacophores. The original pharmacophore for hydroxylations and O-dealkylations uses an interaction between the basic nitrogen in the substrate and Asp301 as the primary binding interaction, while an interaction between an aromatic region in the

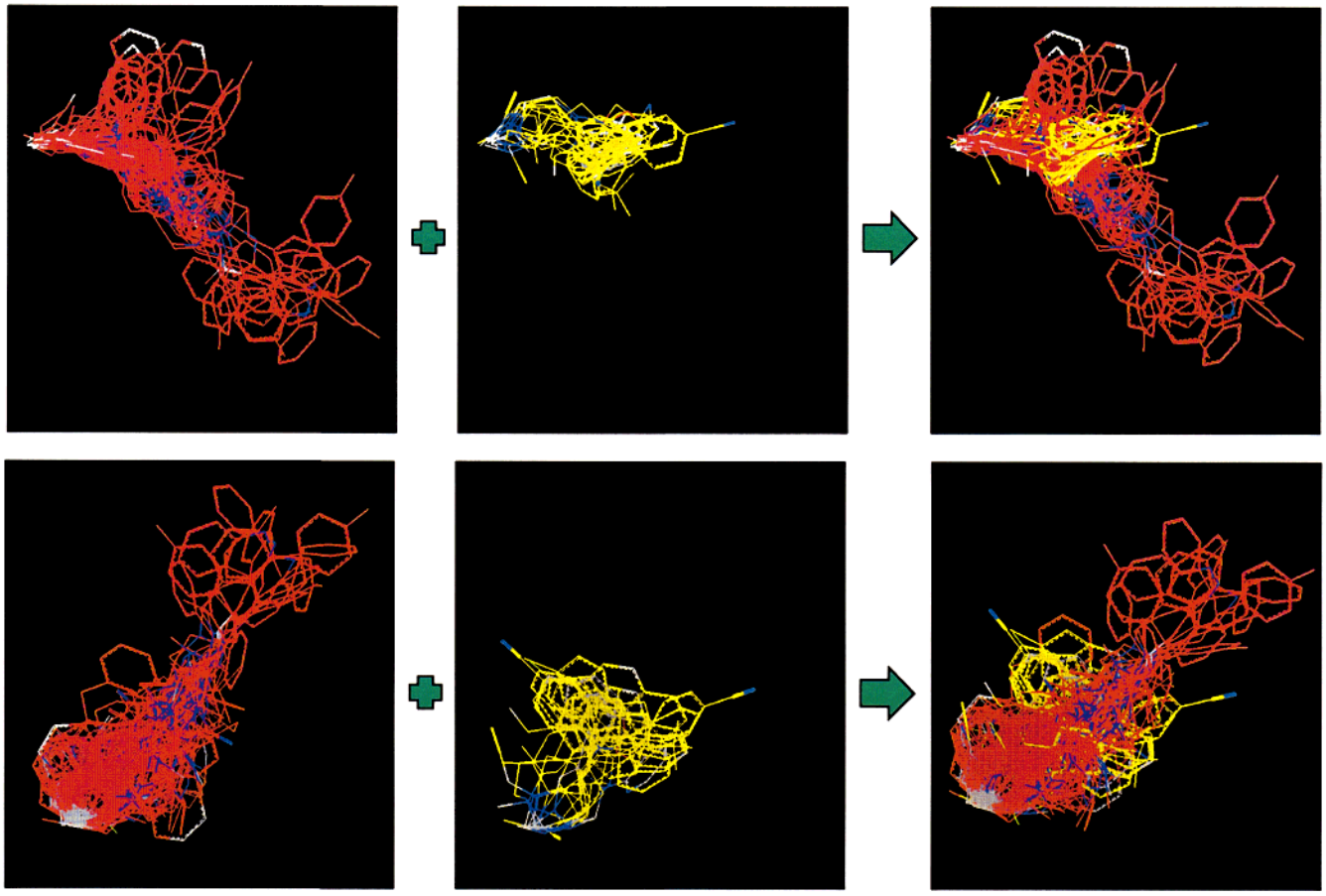

Figure 3. A separate pharmacophore model for CYP2D6 catalyzed N-dealkylations (yellow) was added to the original pharmacophore model for hydroxylations and O-demethylations (red):[7] The combined protein and pharmacophore model now contains two distinct pharmacophores in the protein active site. Protein not shown for clarity. (top) side view, (bottom) top view.

substrates and the side chain of Phe481 provides an additional stabilizing interaction.[7] For the pharmacophore explaining CYP2D6 catalyzed N-dealkylations, the aromatic interaction with Phe481 is the major stabilizing interaction, strengthened by additional binding interactions with Leu121 and Leu213. Amino acids corresponding to Leu121 and Leu213 have been identified as responsible for protein−substrate interactions in CYP108,[22] CYP2A4,[39−42] and CYP2B1,[43−46] respectively. Figure 4 shows one specific example: the orientation leading to N-demethylation of fluoxetine (Prozac) docked in the extended pharmacophore and protein model.

Predicting the Metabolism of Unknown/New Compounds Using the Combined Protein and Pharmacophore Model. 1. Betaxolol (47*R/S*). Initial MO calculations indicated that the most favorable metabolic pathways for **47** would result in hydroxylation at the aliphatic carbon atoms next to any of the oxygen atoms present in the molecule. Taking into account a distance of 5 Å or 7 Å (or possible 10 Å) between a possible site of oxidation and the basic nitrogen atom limited the possibilities to the benzylic site and the two sites adjacent to either oxygen next to the cyclopropane moiety. Only hydroxylation occurring at the benzylic position (green arrow in Figure 2) could be accommodated in the combined CYP2D6 model. The other two metabolic pathways suggested above had the cyclopropane moiety interfering with the heme moiety and were discarded. The experimentally observed metabolism in

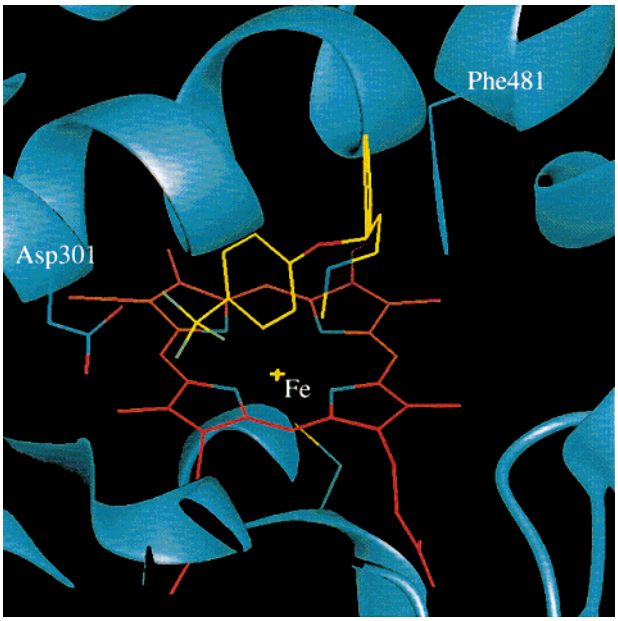

Figure 4. Orientation of fluoxetine (Prozac) leading to N-demethylation in the combined CYP2D6 model. An interaction between the aromatic ring of the substrate and the aromatic side chain of Phe481 stabilizes this orientation, in the absence of an interaction with Asp301.

humans shows the formation of two acid metabolites (major) and the α-hydroxybetaxolol (minor).[47] Although no enzyme is indicated,[47] the formation of the latter

metabolite can be catalyzed by CYP2D6 (in analogy with metoprolol[48]) and corresponds with our predictions, although metabolism of **47** by CYP2D6 has previously been suggested not to be important.[49] As the model is qualitative, no information on relative turnover rates can be obtained, and as a consequence, predicted metabolites might be undetected due to a very low turnover rate. The relative stability of betaxolol compared to metoprolol[47] can be explained by our model, as the cyclopropane moiety in betaxolol results in a less favorable conformation for betaxolol compared to metoprolol.[7] Both the *R*- and the *S*-enantiomer of betaxolol were tested and can be accommodated in the combined protein and pharmacophore model.

2. Fluoxetine (44*R/S*). Fluoxetine was one of the compounds used to construct the N-dealkylation pharmacophore (N-demethylation, see Figure 2, green arrow). Fluoxetine was now used to determine other possible metabolites using the initial pharmacophore (for O-dealkylations and hydroxylations).[7] MO calculations indicated that the most favorable products of both the *R*- and *S*-enantiomers of **44** would be hydroxylated at the aliphatic carbon atoms next to the oxygen or nitrogen atoms present in the molecule or to a lesser extent at the para position of the aromatic ring. Taking into account the above-mentioned distance criteria indicates that the most likely site of oxidation is the para position in the aromatic ring (magenta arrow in Figure 2). This metabolic product has not been reported so far. However, CYP2D6 catalyzed N-demethylation has been detected for fluoxetine (**44**),[50] in line with the MO results indicating hydroxylation next to the basic nitrogen atom and the N-dealkylation pharmacophore (green arrow in Figure 2). As the model is a qualitative model, no information on relative turnover rates can be obtained. In the case of **44**, the turnover rate leading to the para hydroxylated product may be much lower that the turnover rate for the N-demethylation reaction, thus masking the predicted product.

3. Loratidine (48). As in the previous compounds, the MO calculations indicate hydroxylation of the aliphatic carbon atom next to the oxygen atom to result in the energetically most favorable metabolite. The most basic nitrogen atom in **48** is the "pyridine" nitrogen atom. Although this is not a basic nitrogen atom (calculated $pK_a = 3.80 \pm 0.20$[51]), it was used for our predictions. Considering the distance constraints incurred by CYP2D6, two additional possible sites of metabolism were indicated: oxidation of the ring sp^3-carbon atom next to the nitrogen atom and aromatic hydroxylation in the position next to the chlorine atom on the outside of the ring system. These latter two metabolic pathways have to be discarded as orientation of **48** leading to metabolism at those sites resulted in steric clashes with either the protein or the heme moiety. The only possible site of metabolism which complied with 5, 7, or 10 Å between the site of metabolism and the basic nitrogen atom was hydroxylation of the ethyl moiety (green arrow in Figure 2), leading to O-deethylation. This was also the only experimentally observed metabolite for CYP2D6.[52]

4. MPTP (46). MPTP was the template molecule for the N-dealkylation pharmacophore (N-demethylation, green arrow in Figure 2). MPTP was also used to determine other possible metabolites using the original pharmacophore (for O-dealkylations and hydroxylations).[7] MO calculations indicated that hydroxylation of any carbon atom next to the basic nitrogen atom and hydroxylation of the para position of the aromatic ring were energetically favorable and very similar in energy. The only hydroxylation site at approximately 7 Å from the basic nitrogen atom would result in para hydroxylation of the aromatic ring (green arrow in Figure 2). The orientation leading to this metabolite could easily be accommodated in our model. Experimentally this is one of the two metabolites generated by CYP2D6.[31] The experimentally observed main metabolite is the N-demethylation product, which is in line with our MO results and used to construct the N-dealkylation pharmacophore (green arrow in Figure 2).

5. Procainamide (49). The most stable product indicated by the MO calculations is hydroxylated at the aliphatic carbon atom next to the peptidic nitrogen atom. Furthermore, hydroxylation of various positions in the aromatic ring also leads to energetically relatively stable products (1−2 kcal/mol above the most favorable product). Taking into account the distance between the basic nitrogen atom and the site of oxidation and the actual positioning within the active site leads to the prediction of only one possible metabolite, hydroxylated in the aromatic ring next to the amine moiety (magenta arrow in Figure 2). Although radical intermediates for ortho, meta, and para hydroxylation products are very similar in energy (e.g. for **44**, the AM1[29] energies are within 1 kcal/mol), hydroxylation of an aromatic ring would normally take place at the para position, not in the position ortho to the amine. We would therefore not expect this metabolite on steric grounds. So far this metabolite has not been detected experimentally and has to be verified accordingly.

Experimentally only a very unusual metabolite is detected: *N*-hydroxy-procainamide.[53] This is the first ever reported N-hydroxylation reaction catalyzed by CYP2D6. As this is a new pathway, no precedence is present in the training set used to construct our model,[7] and prediction of this metabolite by our current model would therefore not be expected (orange arrow in Figure 2).

6. Ritonavir (50). Initial MO calculations indicated that hydroxylation of aliphatic carbon atoms next to either of the sp^3-oxygen atoms in the compound would result in the most stable products. As there are no basic nitrogen atoms present in **50**, we initially marked **50** as a nonsubstrate. Experimentally, however, a metabolite is found (blue arrow in Figure 2).[54] Reexamination of ritonavir (**50**) in our model indicated a binding orientation which could explain the experimentally observed metabolism (Figure 5).[54] Although no basic nitrogen atom is present in **50**, a variety of interactions are available to maintain **50** in an orientation in the active site which enables metabolism at the experimentally observed position:[54] Ser116 and Gln117 (B′-helix), Glu216 (F-helix), and Asp301 (I-helix) can form hydrogen bonds to **50**, while Phe219 (F-helix) can form an aromatic interaction with the terminal thiazole ring (Figure 5). Ritonavir (**50**), fitted in the active site of the model (Figure 5), is also included in Figures 6 and 7.

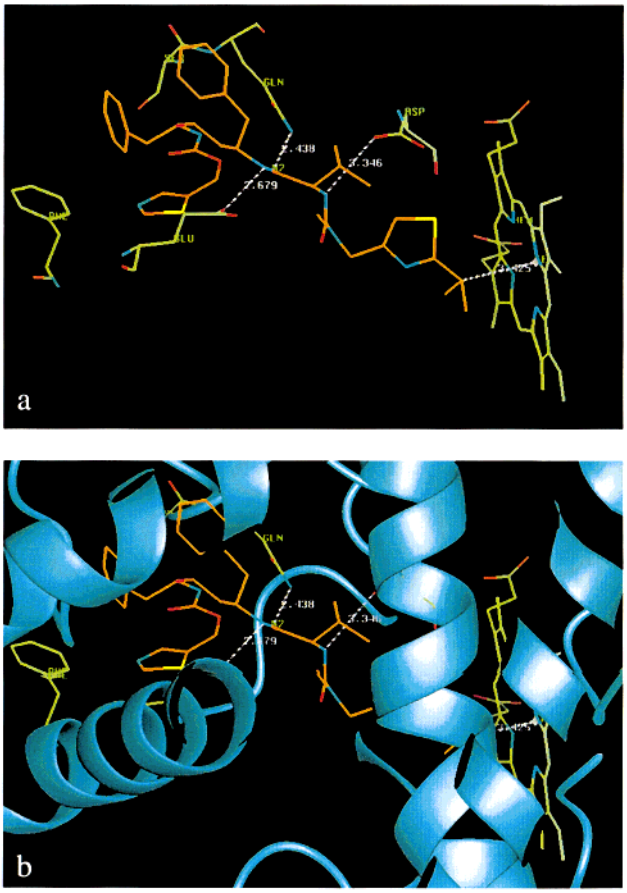

Figure 5. (a) Fit of ritonavir (**50**) in the CYP2D6 model. Amino acids responsible for binding **50** are indicated: Ser116 and Gln117 (B′-helix), Glu216 (F-helix), and Asp301 (I-helix) can form hydrogen bonds to **50**, while Phe219 (F-helix) can form an aromatic interaction with the terminal thiazole ring. (b) Same as part a with secondary structure elements depicted in blue.

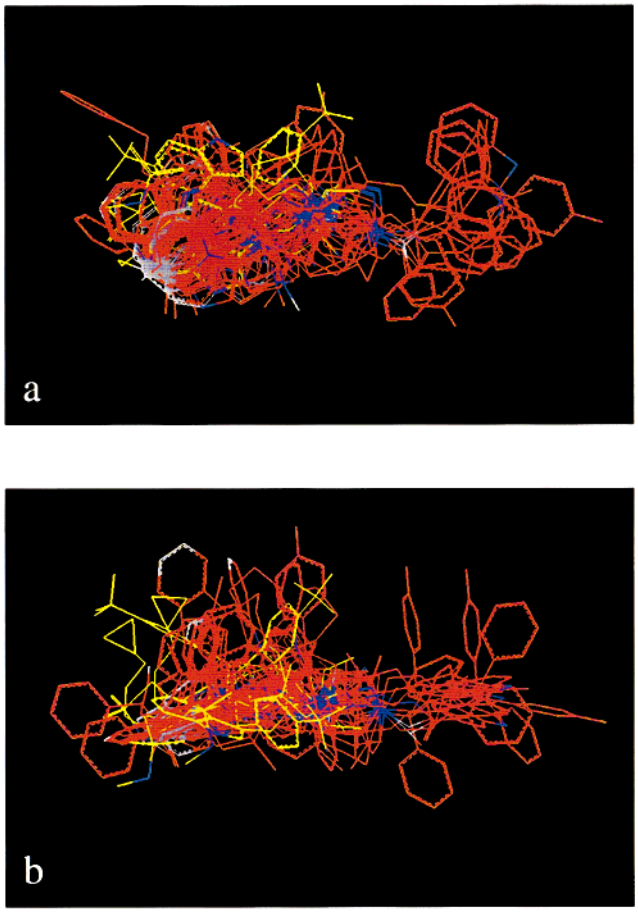

Figure 6. Initial fit in the combined CYP2D6 model: (a) side view, (b) top view. Substrates from the "training set" [7] are shown in red while the "test set" is shown in yellow. Nitrogen atoms are colored blue, while the (possible) site(s) of oxidation are shown in white.

7. Sumatriptan (51). The most energetically favored hydroxylated products of **51** are hydroxylated next to the nitrogen atoms in the molecule, eventually resulting in N-dealkylation products. Of the three sites in the molecule that were approximately 7 Å from the basic nitrogen atom, only the conformation of **51** which would result in N-demethylation of the sulfonamide nitrogen could be accommodated in the active site region of the CYP2D6 model. The orientations of **51** in the active site resulting in aromatic hydroxylation clashed with the heme moiety. However, up until now, no evidence for the involvement of P450s in the metabolism of **51** has been detected,[55] although the sulfonamide N-demethylated product (green arrow in Figure 2) has been observed experimentally.[55] The main enzyme responsible for the metabolism of **51** was found to be monoamine oxidase A (MAO-A).[55] However, metabolism by P450s might be minor and undetectable in the presence of even small amounts of MAO-A. No experimental data based on purified or expressed P450s is available as yet.

Summary of Predictions. Initially, all compounds except **50** were predicted to be metabolized by CYP2D6, based on the combined protein and pharmacophore model. All conformations of these compounds leading to metabolism at the predicted sites (indicated with green and magenta arrows in Figure 2) are shown as yellow structures in Figures 6 and 7. Ritonavir (**50**) was initially not predicted as a CYP2D6 substrate due to the lack of basic nitrogen atoms in the molecule. There was no precedence in the training set used to construct our model[7] for this type of molecule, and for this reason this metabolite would not be expected to be predicted by our current model. However, upon close examination, the metabolism of ritonavir (**50**) could be accommodated into the current model (Figure 2, blue arrow). Although no basic nitrogen atom is present in the molecule, a combination of interactions with amino acids from several structural elements of CYP2D6 can compensate for this (e.g. weaker interactions with Ser116, Gln117, Glu216, Phe219, and Asp301 instead of a strong interaction (acid−base) with either Glu216 or Asp301 alone[7]).

Computational results for these metabolic pathways are shown in Table 2. Figure 6 shows all compounds fitted into the overall model without optimizing the compounds in the protein. Figure 7 shows the same compounds after minimization inside the CYP2D6 active site (see Computational Methods). The most remarkable differences are visible when examining the pharmacophore model from a top view (compare Figures 6b and 7b). As indicated previously,[7] the region around the site of oxidation is slightly less coplanar, and the substrates extending toward the top (see side view Figures 6a and 7a) become more tightly clustered due to an interaction with Phe481. Substrates which extend from the overall volume of the pharmacophore model

Table 2. CYP2D6 Substrates Used in the Model, Their *Predicted* Metabolic Pathways, Their Distances between Site(s) of Oxidation and Basic Nitrogen Atom, and *Experimental Verification* of the Predictions

no.[7,27]	name	predicted pathway(s)	distance (Å)	experimentally observed?	ref
47*R/S*	betaxolol	benzylic hydroxylation	8.41 (*R*/*S*)	yes[a]	47
44*R/S*	fluoxetine	para hydroxylation	7.66 (*R*) 7.49 (*S*)	no	50
		N-demethylation	NA[b]	yes	
48	loratidine	O-dealkylation	7.77	yes	52
46	MPTP	para hydroxylation	7.29	yes	31
		N-demethylation	NA[b]	yes	
49	procainamide	aromatic hydroxylation	7.78	no[c]	53
50	ritonavir	none		*c,d*	54
51	sumatriptan	N-demethylation	7.92	yes[e]	55

[a] Although this metabolite is detected in humans, no indication was given for the enzyme responsible for this minor metabolite.[47] [b] NA: not applicable. [c] Experimentally observed product not predicted. [d] Experimentally observed product could be rationalized by the model. [e] Although this metabolite was detected, the enzyme responsible for this metabolite is not known.[55]

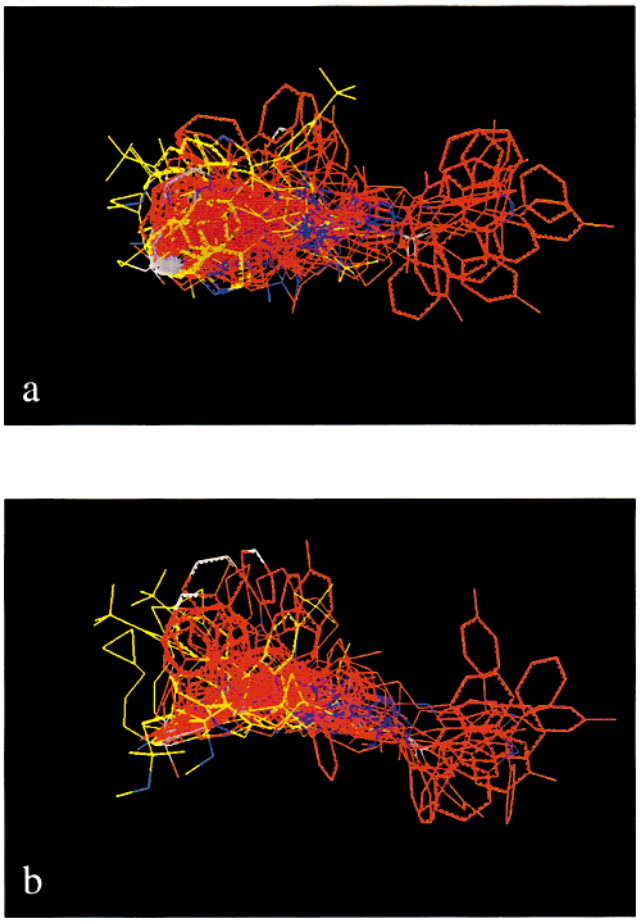

Figure 7. Orientations of the various predicted substrates are shown after (constrained) geometry optimization within the CYP2D6 active site: (a) side view, (b) top view. Each substrate was independently energy minimized in the active site of the protein model starting from the orientation shown in Figure 6. Substrates from the "training set"[7] are shown in red while the "test set" is shown in yellow. Nitrogen atoms are colored blue, while the (possible) site(s) of oxidation are shown in white.

(Figure 6b) are incorporated in distinct groups of substrates after minimization in the protein (Figure 7b). The side view confirms that the overlay of the substrates is improved by minimization in the protein (compare Figures 6a and 7a).

When all test compounds were subsequently submitted to an AM1 geometry optimization (starting from the bound structures (Figure 7)), the geometry of the substrates changed only slightly. The energy differences between these AM1 optimized geometries and the AM1 energies for the global minimum were less than 4.2 kcal/mol. As there were no significant conformational changes on minimizing the test set in the absence of the protein, the conformations resulting from minimization within the protein are low-energy conformations and not sterically constrained high-energy conformations.

Conclusions

The initial combined pharmacophore and protein model[7] has now been extended with a second pharmacophore in order to explain CYP2D6 catalyzed N-dealkylation reactions, which have become accepted metabolic pathways.[24] A group of 14 experimentally verified N-dealkylation reactions form the basis of this second pharmacophore (Figure 1). The combined model now contains 51 substrates catalyzed by CYP2D6, describing 72 different metabolic pathways.

As stated before, a combination of pharmacophore modeling and protein modeling results in a well-defined and reproducible model which will take into account not only the similarities between the various substrates but also the steric and electronic properties of the surrounding enzyme. As shown above, this can mean that several pharmacophores (for different metabolic pathways, Figure 3) have to be combined. Molecular orbital calculations can identify the chemically most likely intermediates and products based on internal energies; however, the steric and electronic influences of the protein, which distinguish the catalyzed reaction from the chemical reaction, are ignored. When predicting the possible metabolism of newly designed compounds, these calculations are very useful in indicating the most reactive atoms of the compound and suggest possible sites of metabolism. With the addition of the N-dealkylation pharmacophore to the original combined pharmacophore and protein model, all currently known metabolic pathways catalyzed by CYP2D6 can be explained by the extended model.

For the well-established CYP2D6 metabolic routes, the predictive value of the current combined protein and pharmacophore model is good. The known metabolites were all predicted by the model, except the highly unusual metabolism of procainamide (**49**, orange arrow in Figure 2) and ritonavir (**50**, blue arrow in Figure 2). Two possible sites of metabolism that have not been detected experimentally (yet) have also been predicted

by the current model (Figure 2 magenta arrows), one of which (metabolism of **49**) would, however, not be expected on steric grounds. These metabolites have to be verified experimentally in order to determine whether the model made incorrect predictions or that the metabolites have so far eluded detection. If the experiments fail to identify the predicted metabolites, the model has to be modified to incorporate these findings. As the model is qualitative, no information on relative turnover rates can be obtained, and as a consequence, predicted metabolites might be undetected due to a very low turnover rate (e.g. **44**). Should the metabolites be detected experimentally, this would indicate the model's ability to guide experiments. Ritonavir (**50**) was initially discounted as being a CYP2D6 substrate due to the lack of basic nitrogen atoms in the molecule. However, its metabolism could be accommodated into the current model as several weaker interactions between protein and **50** can compensate for the absence of the interaction between a basic nitrogen atom and Asp301.

P450 models, like the one presented here, have wide applications in the drug design process which may allow prediction and elimination of polymorphic metabolism and drug−drug interactions. This novel input into the design process may help to achieve better quality drug candidates, resulting in lower attrition rates due to adverse metabolic properties. Predictions relevant to guide drug development can now be made for both the common CYP2D6 metabolic pathways as well as for the less common ones.

References

(1) Nelson, D. R.; Koymans, L.; Kamataki, T.; Stegeman, J. J.; Feyereisen, R.; Waxman, D. J.; Waterman, M. R.; Gotoh, O.; Coon, M. J.; Estabrook, R. W.; Gunsalus, I. C.; Nebert, D. W. P450 superfamily: update on new sequences, gene mapping, accession numbers and nomenclature. *Pharmacogenetics* **1996**, *6*, 1−42.

(2) Daly, A. K.; Brockmöller, J.; Broly, F.; Eichelbaum, M.; Evans, W. E.; Gonzalez, F. J.; Huang, J. D.; Idle, J. R.; Ingelman-Sundberg, M.; Ishizaki, T.; Jacqz-Aigrain, E.; Meyer, U. A.; Nebert, D. W.; Steen, V. M.; Wolf, C. R.; Zanger, U. M. Nomenclature for human *CYP2D6* alleles. *Pharmacogenetics* **1996**, *6*, 193−201.

(3) Koymans, L. M. H.; Vermeulen, N. P. E.; van Acker, S. A. B. E.; te Koppele, J. M.; Heykants, J. J. P.; Lavrijsen, K.; Meuldermans, W.; Donné-Op den Kelder, G. M. A predictive model for substrates of cytochrome P-450-debrisoquine (2D6). *Chem. Res. Toxicol.* **1992**, *5*, 211−219.

(4) Strobl, G. R.; von Kreudener, S.; Stöckigt, J.; Guengerich, F. P.; Wolff, T. Development of a pharmacophore for inhibition of human liver cytochrome P-450 2D6: molecular modelling and inhibition studies. *J. Med. Chem.* **1993**, *36*, 1136−1145.

(5) de Groot, M. J.; Bijloo, G. J.; Martens, B. J.; van Acker, F. A. A.; Vermeulen, N. P. E. A refined substrate model for human cytochrome P450 2D6. *Chem. Res. Toxicol.* **1997**, *10*, 41−48.

(6) Lewis, D. F. V.; Eddershaw, P. J.; Goldfarb, P. S.; Tarbit, M. H. Molecular modelling of cytochrome P4502D6 (CYP2D6) based on an alignment with CYP102: structural studies on specific CYP2D6 substrate metabolism. *Xenobiotica* **1997**, *27*, 319−340.

(7) de Groot, M. J.; Ackland, M. J.; Horne, V. A.; Alex, A. A.; Jones, B. C. Novel approach to predicting P450 mediated drug metabolism. The development of a combined protein and pharmacophore model for CYP2D6. *J. Med. Chem.* **1999**, *42*, 1515−1524.

(8) Wolff, T.; Distlerath, L. M.; Worthington, M. T.; Groopman, J. D.; Hammons, G. J.; Kadlubar, F. F.; Prough, R. A.; Martin, M. V.; Guengerich, F. P. Substrate specificity of human liver cytochrome P-450 debrisoquine hydroxylase probed using immunochemical inhibition and chemical modeling. *Cancer Res.* **1985**, *45*, 2116−2122.

(9) Meyer, U. A.; Gut, J.; Kronbach, T.; Skoda, C.; Meier, U. T.; Catin, T.; Dayer, P. The molecular mechanism of two common polymorphisms of drug oxidation. Evidence for functional changes in cytochrome P-450 isozymes catalysing bufuralol and mephenytoin oxidation. *Xenobiotica* **1986**, *16*, 449−464.

(10) Islam, S. A.; Wolf, C. R.; Lennard, M. S.; Sternberg, M. J. E. A three-dimensional molecular template for substrates of human cytochrome P450 involved in debrisoquine 4-hydroxylation. *Carcinogenesis* **1991**, *12*, 2211−2219.

(11) de Groot, M. J.; Bijloo, G. J.; Hansen, K. T.; Vermeulen, N. P. E. Computer prediction and experimental validation of cytochrome P450−2D6 dependent oxidation of GBR 12909 (1-[2-[bis-(4-fluorophenyl)methoxy]ethyl]-4-(3-phenylpropyl)piperazine). *Drug Metab. Dispos.* **1995**, *23*, 667−669.

(12) de Groot, M. J.; Bijloo, G. J.; van Acker, F. A. A.; Fonseca Guerra, C.; Snijders, J. G.; Vermeulen, N. P. E. Extension of a predictive substrate model for human cytochrome P4502D6. *Xenobiotica* **1997**, *27*, 357−368.

(13) Koymans, L. M. H.; Vermeulen, N. P. E.; Baarslag, A.; Donné-Op den Kelder, G. M. A preliminary 3D model for cytochrome P450 2D6 constructed by homology model building. *J. Comput.-Aided Mol. Des.* **1993**, *7*, 281−289.

(14) Lewis, D. F. V. Three-dimensional models of human and other mammalian microsomal P450s constructed from an alignment with CYP102 ($P450_{bm3}$). *Xenobiotica* **1995**, *25*, 333−366.

(15) Modi, S.; Paine, M. J.; Sutcliffe, M. J.; Lian, L. Y.; Primrose, W. U.; Wolf, C. R.; Roberts, G. C. K. A model for human cytochrome P_{450} 2D6 based on homology modeling and NMR studies of substrate binding. *Biochemistry* **1996**, *35*, 4540−4550.

(16) de Groot, M. J.; Vermeulen, N. P. E.; Kramer, J. D.; van Acker, F. A. A.; Donné-Op den Kelder, G. M. A three-dimensional protein model for human cytochrome P450 2D6 based on the crystal structures of P450 101, P450 102 and P450 108. *Chem. Res. Toxicol.* **1996**, *9*, 1079−1091.

(17) Ellis, S. W.; Rowland, K.; Ackland, M. J.; Rekka, E.; Simula, A. P.; Lennard, M. S.; Wolf, C. R.; Tucker, G. T. Influence of amino acid residue 374 of cytochrome P450 2D6 (CYP2D6) on the regio- and enantioselective metabolism of metoprolol. *Biochem. J.* **1996**, *316*, 647−654.

(18) Poulos, T. L.; Finzel, B. C.; Gunsalus, I. C.; Wagner, G. C.; Kraut, J. The 2.6-Å crystal structure of *Pseudomonas putida* cytochrome P-450. *J. Biol. Chem.* **1985**, *260*, 16122−16130.

(19) Poulos, T. L.; Finzel, B. C.; Howard, A. J. High-resolution crystal structure of cytochrome P450cam. *J. Mol. Biol.* **1987**, *195*, 687−700.

(20) Ravichandran, K. G.; Boddupalli, S. S.; Hasemann, C. A.; Peterson, J. A.; Deisenhofer, J. Crystal structure of hemoprotein domain of P450 μ_B-3, a prototype for microsomal P450s. *Science* **1993**, *261*, 731−736.

(21) Li, H.; Poulos, T. L. Modeling protein-substrate interactions in the heme domain of cytochrome $P450_{BM-3}$. *Acta Crystallogr. Sect. D-Biol. Crystallogr.* **1995**, *51*, 21−32.

(22) Hasemann, C. A.; Ravichandran, K. G.; Peterson, J. A.; Deisenhofer, J. Crystal structure and refinement of cytochrome $P450_{terp}$ at 2.3 Å resolution. *J. Mol. Biol.* **1994**, *236*, 1169−1185.

(23) de Groot, M. J.; Vermeulen, N. P. E. Modeling the active site of cytochrome P450s and glutathione *S*-transferases, two of the most important biotransformation enzymes. *Drug Metab. Rev.* **1997**, *29*, 747−799.

(24) Coutts, R. T.; Su, P.; Baker, G. B. Involvement of CYP2D6, CYP3A4, and other cytochrome P-450 isozymes in N-dealkylation reactions. *J. Pharmacol. Toxicol. Methods* **1994**, *31*, 177−186.

(25) A diverse set of substrates was selected randomly from the literature from compounds not included in the training set.

(26) Wave function Inc., Irvine, CA 92715. Spartan, 1996, SGI version 4.1.1 OpenGL.

(27) The numbering of substrates is continued from the first part of this publication (ref 7).

(28) Conformational search using the SYBYL force field employing the genetic algorithm, without geometry optimization (popsize = 150−250 depending on number of rotable bonds). Of the resulting conformers, all conformers within 25 kcal/mol from the lowest energy were geometry optimized using AM1 (optcycle = 1000, maxcycle = 1000).

(29) Dewar, M. J. S.; Zoebisch, E. G.; Healy, E. F.; Stewart, J. J. P. AM1: a new general purpose quantum mechanical molecular model. *J. Am. Chem. Soc.* **1985**, *107*, 3902−3909.

(30) Geometry optimization using AM1 (optcycle = 1000, maxcycle = 1000).

(31) Modi, S.; Gilham, D. E.; Sutcliffe, M. J.; Lian, L.-Y.; Primrose, W. U.; Wolf, C. R.; Roberts, G. C. K. 1-Methyl-4-phenyl-1,2,3,6-tetrahydropyridine as a substrate of cytochrome P450 2D6: allosteric effects of NADPH-cytochrome P450 reductase. *Biochemistry* **1997**, *36*, 4461−4470.

(32) The site of oxidation and the aromatic rings of the substrates were superimposed.

(33) Tripos Inc., St. Louis, MO 63144-2913. SYBYL, 1997; Version 6.4.

(34) Minimization options: SYBYL force field, Powell minimization with standard minimize details. Termination on gradient <0.1 kcal/(mol·Å), with as many iterations as required for convergence. Constraint: iron−site of oxidation 3.0 Å (constant = 200

kcal/(mol·Å^2)). Torsional constraints to keep the aromatic rings planar (constant = 5 kcal/(mol·Å^2)) were used. Starting orientations have aromatic ring in substrate coplanar with aromatic ring of Phe481.

(35) Minimization options: SYBYL force field, Powell minimization with standard minimize details. Termination on gradient <0.1 kcal/(mol·Å), with as many iterations as required for convergence. Constraints: iron−site of oxidation 3.0 Å (constant = 200 kcal/mol·Å^2) and basic nitrogen atom−Asp301 carboxylate oxygen or basic nitrogen atom−Glu216 carboxylate oxygen 2.7 Å (constant = 100 kcal/mol·Å^2).

(36) The model which has the methyl of MPTP closest to the heme was selected.

(37) Singh, J.; Thornton, J. M. *Atlas of Protein Side-Chain Interactions*; IRL Press: Oxford, 1992; Vol. 1.

(38) Singh, J.; Thornton, J. M. *Atlas of Protein Side-Chain Interactions*; IRL Press: Oxford, 1992; Vol. 2.

(39) Lindberg, R. L.; Negishi, M. Alteration of mouse cytochrome $P450_{coh}$ substrate specificity by mutation of a single amino acid residue. *Nature* **1989**, *399*, 632−634.

(40) Juvonen, R. O.; Iwasaki, M.; Negishi, M. Structural function of residue-209 in coumarin 7-hydroxylase (P450coh). Enzyme-kinetic studies and site-directed mutagenesis. *J. Biol. Chem.* **1991**, *266*, 16431−16435.

(41) Iwasaki, M.; Darden, T. A.; Pedersen, L. G.; Davis, D. G.; Juvonen, R. O.; Sueyoshi, T.; Negishi, M. Engineering mouse P450coh to a novel corticosterone 15α-hydroxylase and modeling steroid-binding orientation in the substrate pocket. *J. Biol. Chem.* **1993**, *268*, 759−762.

(42) Iwasaki, M.; Lindberg, R. L. P.; Juvonen, R. O.; Negishi, M. Site-directed mutagenesis of mouse steroid 7α-hydroxylase (cytochrome $P\text{-}450_{7\alpha}$): role of residue-209 in determining steroid-cytochrome P-450 interaction. *Biochem. J.* **1993**, *291*, 569−573.

(43) Szklarz, G. D.; Ornstein, R. L.; Halpert, J. P. Application of 3-dimensional homology modeling of cytochrome P450 2B1 for interpretation of site-directed mutagenesis results. *J. Biomol. Struct. Dyn.* **1994**, *12*, 61−78.

(44) Luo, Z.; He, Y. A.; Halpert, J. R. Role of residues 363 and 206 in conversion of cytochrome P450 2B1 from steroid 16-hydroxylase to a 15α-hydroxylase. *Arch. Biochem. Biophys.* **1994**, *309*, 52−57.

(45) He, Y.; Luo, Z.; Klekotka, P. A.; Burnett, V. L.; Halpert, J. R. Structural determinants of cytochrome P450 2B1 specificity: evidence for five substrate recognition sites. *Biochemistry* **1994**, *33*, 4419−4424.

(46) He, Y. Q.; He, Y. A.; Halpert, J. R. *Escherichia coli* expression of site-directed mutants of cytochrome P450 2B1 from six substrate recognition sites: substrate specificity and inhibitor selectivity studies. *Chem. Res. Toxicol.* **1995**, *8*, 574−579.

(47) Wong, Y. W. J.; Ludden, T. M. Determination of betaxolol and its metabolites in blood and urine by high-performance liquid chromatochraphy with fluorimetric detection. *J. Chromatogr.* **1990**, *534*, 161−172.

(48) Mautz, D. S.; Nelson, W. L.; Shen, D. D. Regioselective and stereoselective oxidation of metoprolol and bufuralol catalyzed by microsomes containing cDNA-expressed human P4502D6. *Drug Metab. Dispos.* **1995**, *23*, 513−517.

(49) Ferrari, S.; Leemann, T.; Dayer, P. The role of lipophilicity in the inhibition of polymorphic cytochrome P450IID6 oxidation by beta-blocking agents in vitro. *Life Sci.* **1991**, *48*, 2259−2265.

(50) Hamelin, B. A.; Turgeon, J.; Vallee, F.; Belanger, P.-M.; Paquet, F.; LeBel, M. The disposition of fluoxetine but not sertraline is altered in poor metabolizers of debrisoquin. *Clin. Pharmacol. Ther.* **1996**, *60*, 512−521.

(51) ACD (Advanced Chemistry Development Inc.), 133 Richmond St West, Suite 605, Toronto, Canada., ACD, 1998, 3.5 (09 April 1998).

(52) Yumibe, N.; Huie, K.; Chen, K.-J.; Snow, M.; Clement, R. P.; Cayen, M. N. Identification of human liver cytochrome P450 enzymes that metabolize the nonsedating antihisamine loratadine. Formation of descarboethoxylaratadine by CYP3A4 and CYP2D6. *Biochem. Pharmacol.* **1996**, *51*, 165−172.

(53) Lessard, E.; Fortin, A.; Belanger, P. M.; Beaune, P.; Hamelin, B. A.; Turgeon, J. Role of CYP2D6 in the N-hydroxylation of procainamide. *Pharmacogenetics* **1997**, *7*, 381−390.

(54) Kumar, G. N.; Rodrigues, A. D.; Buko, A. M.; Denissen, J. F. Cytochrome P450-mediated metabolism of the HIV-1 protease inhibitor ritonavir (ABT-538) in human liver microsomes. *J. Pharmacol. Exp. Ther.* **1996**, *277*, 423−431.

(55) Dixon, C. M.; Park, G. R.; Tarbit, M. H. Characterization of the enzyme responsible for the metabolism of Sumatriptan in human liver. *Biochem. Pharmacol.* **1994**, *47*, 1253−1257.

(56) Coutts, R. T.; Bach, M. V.; Baker, G. B. Metabolism of amitriptyline with CYP2D6 expressed in a human cell line. *Xenobiotica* **1997**, *27*, 33−47.

(57) Ghahramani, P.; Ellis, S. W.; Lennard, M. S.; Ramsay, L. E.; Tucker, G. T. Cytochromes P450 mediating *N*-demethylation of amitriptyline. *Br. J. Clin. Pharmacol.* **1997**, *43*, 137−144.

(58) Olesen, O. V.; Linnet, K. Metabolism of the tricyclic antidepressant amitriptyline by cDNA-expressed human cytochrome P450 enzymes. *Pharmacology* **1997**, *55*, 235−243.

(59) Rochat, B.; AMey, M.; Gillet, M.; Meyer, U. A.; Baumann, P. Identification of three cytochrome P450 isozymes involved in N-demethylation of citaolpram enantiomers in human liver microsomes. *Pharmacogenetics* **1997**, *7*, 1−10.

(60) Linnet, K.; Olesen, O. V. Metabolism of clozapine by cDNA-expressed human cytochrome P450 enzymes. *Drug Met. Disp.* **1997**, *25*, 1379−1382.

(61) Grace, J. M.; Kinter, M. T.; Macdonald, T. L. Atypical metabolism of deprenyl and its enantiomer, (S)-(+)-N,α-dimethyl-N-propynylphenethylamine, by cytochrome P450 2D6. *Chem. Res. Toxicol.* **1994**, *7*, 286−290.

(62) Coutts, R. T.; Su, P.; Baker, G. B.; Daneshtalab, M. Metabolism of imipramine in vitro by isozyme CYP2D6 expressed in a human cell line, and observations on metabolite stability. *J. Chromatogr. Biomed. Appl.* **1993**, *615*, 265−272.

(63) Su, P.; Coutts, R. T.; Baker, G. B.; Daneshtalab, M. Analysis of imipramine and three metabolites produced by isozyme CYP2D6 expressed in a human cell line. *Xenobiotica* **1993**, *23*, 1289−1298.

(64) Lin, L. Y.; di Stefano, E. W.; Schmitz, D. A.; Hsu, L.; Ellis, S. W.; Lennard, M. S.; Tucker, G. T.; Cho, A. K. Oxidation of methamphetamine and methylenedioxymetamphetamine by CYP2D6. *Drug Metab. Dispos.* **1997**, *25*, 1059−1064.

(65) Geertsen, S.; Foster, B. C.; Wilson, D. L.; Cyr, T. D.; Casley, W. Metabolism of methoxyphenamine and 2-methoxyamphetamine in P4502D6-transfected cells and cell preparations. *Xenobiotica* **1995**, *25*, 895−906.

(66) Koyama, E.; Chiba, K.; Tani, M.; Ishizaki, T. Identification of human cytochrome P450 isoforms involved in the stereoselective metabolism of mianserin enantiomers. *J. Pharmacol. Exp. Ther.* **1996**, *278*, 21−30.

(67) Dahl, M. L.; Voortman, G.; Alm, C.; Elwin, C. E.; Delbressine, L.; Vos, R.; Bogaards, J. J. P.; Bertilsson, L. In vitro and in vivo studies on the disposition of mirtazapine in humans. *Clin. Drug Invest.* **1997**, *13*, 37−46.

(68) Gilham, D. E.; Cairns, W.; Paine, M. J. I.; Modi, S.; Poulsom, R.; Roberts, G. C. K.; Wolf, C. R. Metabolism of MPTP by cytochrome P4502D6 and the demonstration of 2D6 mRNA in human foetal and adult brain by in situ hybridization. *Xenobiotica* **1997**, *27*, 111−125.

(69) Olesen, O. V.; Linnet, K. Hydroxylation and demethylation of the tricyclic antidepressant nortriptyline by cDNA-expressed human cytochrome P-450 isozymes. *Drug Metab. Dispos.* **1997**, *25*, 740−744.

(70) Yoshimoto, K.; Echizen, H.; Chiba, K.; Tani, M.; Ishizaki, T. Identification of human CYP isoforms involved in the metabolism of propranolol enantiomers. *N*-desisopropylation is mediated mainly by CYP1A2. *Br. J. Clin. Pharmacol.* **1995**, *39*, 421−431.

(71) Rowland, K.; Ellis, S. W.; Lennard, M. S.; Tucker, G. T. Variable contribution of CYP2D6 to the N-dealkylation of S-(−)-propranolol by human liver micriosomes. *Br. J. Clin. Pharmacol.* **1996**, *42*, 390−393.

JM991058V